Engineering Structures 215 (2020) 110670

Contents lists available at ScienceDirect

Engineering Structures

journal homepage: www.elsevier.com/locate/engstruct

Efficient nonlinear modeling of strong wood frame shear walls for mid-rise buildings

Xavier Estrella[a,b,c,*], Pablo Guindos[b,c], José Luis Almazán[b], Sardar Malek[a,1]

[a] School of Civil and Environmental Engineering, University of Technology Sydney, 81 Broadway Street, Ultimo NSW 2007, Australia
[b] Department of Structural and Geotechnical Engineering, Pontificia Universidad Católica de Chile, Av. Vicuña Mackenna, Santiago 7820436, Chile
[c] UC Center for Wood Innovation (CIM), Pontificia Universidad Católica de Chile, Av. Vicuña Mackenna, Santiago 7820436, Chile

ARTICLE INFO

Keywords:
Wood frame construction
Timber buildings
Nonlinear modeling
Light-frame shear walls

ABSTRACT

Designing mid-rise timber buildings in seismic areas requires stronger wood frame shear walls compared to those required in low-rise structures. Despite some experimental research has been conducted lately to demonstrate the difference between the lateral response of such 'strong' walls and conventional ones, investigations on numerical models that could reproduce their nonlinear behavior under seismic loads are limited. This paper presents an efficient nonlinear modeling approach to better understand such behavior under large displacement demands. The numerical model was validated using a set of twelve real-scale experiments. The model predictions showed an accuracy of ± 8% for 1:1 walls and proved its suitability to capture the post-peak phenomena such as force degradation, stiffness degradation, and pinching. For the aspect ratios investigated, anchorage system demands were found to remain 50% below the failure capacity. It was also shown that redesigning the nailing pattern can increase the capacity of strong wood frame walls by up to 10%. Finally, the application of the developed numerical model in calibrating simpler single-degree-of-freedom (SDOF) models for reproducing the hysteretic response of strong walls was discussed. Since shear behavior governs the deformation of wood frame walls, the parameters of the SDOF model can be defined proportionally to the wall length. This may be used as a simple and easy-to-use tool to compute the dynamic behavior of mid-rise timber buildings with strong wood frame walls.

1. Introduction

Over the past few decades, wood frame structures have gained a significant presence in low-rise construction throughout North America, Europe, and Oceania. Recent data [1] show a promising future for multi-story timber buildings worldwide for the years to come. When wood frame structures are subjected to earthquake loads, shear walls are commonly employed as the primary component of the lateral resisting system. Typically, a wood frame shear wall consists of a 1.2–2.4 m long wood frame with 38 × 89 mm (2″ × 4″) interior studs spaced at 400 mm on center, double end studs, single members for the top and sole plate, and conventional corner hold-downs to prevent overturning of the wall.

In a low-rise wood frame structure, the lateral resistance is usually provided by 9 to 11 mm thick oriented strand board (OSB) panels on one side of the wall, with nails spaced at 150 mm on center along all panel edges and 300 mm for interior studs, as shown in Fig. 1(a). However, for mid-rise structures, a wall configuration of higher capacity is often required to resist the larger vertical and horizontal forces due to the increased gravitational and seismic loads. This higher capacity configuration is referred to as 'strong' throughout this paper. A strong wood shear wall usually consists of 38 × 135 mm (2″ × 6″) framing members, sturdy end studs, stronger hold-down devices, OSB panels on both sides of the wall, and a smaller nail spacing both along the panel edges and interior studs, as shown in Fig. 1(b). Previous research has shown that these practices may also increase the damping ratio of the walls [2].

1.1. State of the art: experimental programs

Understanding the structural behavior of strong wood frame shear walls is a key step for the development of mid-rise timber buildings in seismic countries, since the current building codes and design procedures have been developed based on previous works conducted on

* Corresponding author at: School of Civil and Environmental Engineering, University of Technology Sydney, 81 Broadway Street, Ultimo NSW 2007, Australia.
E-mail address: exestrella@uc.cl (X. Estrella).
[1] Present address: Department of Civil Engineering, University of Victoria, 3800 Finnerty Rd, Victoria, BC, Canada.

https://doi.org/10.1016/j.engstruct.2020.110670
Received 29 August 2019; Received in revised form 18 February 2020; Accepted 14 April 2020

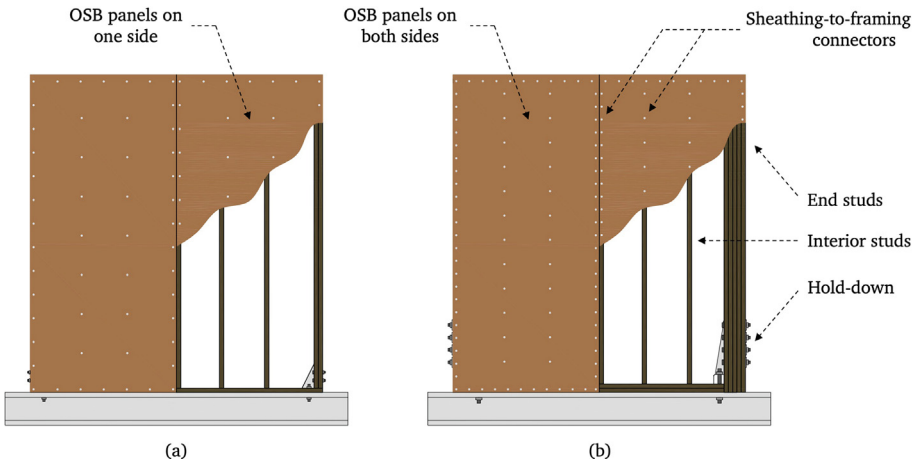

Fig. 1. Schematic configuration of (a) conventional and (b) strong wood frame shear walls.

conventional walls. However, investigations on strong wood frame walls are scarce. van de Lindt et al. [3] studied the experimental seismic response of a full-scale, six-story, wood frame apartment building at the world's largest shake table in Miki, Japan. The results showed a good behavior of the building even under high seismic demands, with a maximum averaged interstory drift of 2% and only minor nonstructural damage. Seim et al. [4] carried out a comparative study of the lateral behavior of wood frame walls with OSB and gypsum fiber board (GFB) panels. Eight 2.5 × 2.5 m strong walls were tested at the testing facilities of the University of Kassel under vertical and horizontal (monotonic and cyclic) load. The specimens were sheathed with two 1.25 × 2.5 m panels on both sides, which were attached to the framing with 2.8 × 65 mm nails spaced at 75 mm. Results showed that there is no significant difference in the performance of walls with thick GFB panels (18 mm thick) and standard OSB ones (10 or 18 mm thick) under lateral loads. However, walls constructed with thin GFB panels (10 mm thick) had a slightly lower performance in terms of maximum load-bearing capacity, ultimate deformation, ductility, and equivalent damping. Marzaleh et al. [5] investigated the monotonic response of wood frame shear walls with strong anchorage and sturdy end studs subjected to vertical load and bending moment, reproducing the expected load conditions in multi-story buildings. Three racking tests were conducted under different load conditions, and a substantial increase in shear resistance and stiffness was found for strong walls.

Recently, Guíñez et al. [6] studied the monotonic and cyclic lateral response of strong wood frame walls with different lengths and nail spacings. It was found that strong walls have an increased capacity and delayed stiffness degradation. Furthermore, the results showed that the current design guidelines underestimate the shear strength and overestimate the stiffness of strong wood frame walls.

1.2. State of the art: numerical modeling

Since real-scale tests are usually complex, expensive, and time-consuming, a more viable approach to study the behavior of wood frame walls is through virtual testing using numerical models. Much research efforts have been devoted to the development of models capable of predicting the monotonic and cyclic response of wood frame walls in the past decades. In the early 1980s, Easley et al. [7] developed a set of analytical expressions based on test results to predict the stiffness and force–displacement relationship of wood frame walls. Results showed that the model is mainly accurate in the linear range of the response. Itani and Cheung [8] employed a detailed FEM model to study the nonlinear response of wood frame diaphragms. In their model, the studs and the sheathing panels were represented by beam and plane-stress elements, and nonlinear springs were used to represent the sheathing-to-framing connections. Over time, more detailed FEM models have also been developed by various researchers [9–13]. As the wall response is mainly governed by the nonlinear shear behavior of the sheathing-to-framing connections [14], the global force–displacement relationship can be well-predicted employing simpler models, as the one proposed by Gupta and Kuo [15]. They studied the effect of uplifting in vertical studs through a five degree-of-freedom model for single-story shear walls (with two extra degrees of freedom for each additional story). This allowed them to gain knowledge about the effect of vertical load on the cyclic response of walls.

Due to the great damage observed in wood frame structures after the Northridge earthquake, the Consortium of Universities for Research in Earthquake Engineering (CUREE)–Caltech Woodframe Research Project was initiated to improve the wood construction engineering in 1998 [16]. As part of this project, Folz and Filiatrault [17] proposed a simplified mechanistic model to predict the in-plane behavior of wood frame walls under quasi-static loading. The model's numerical formulation was based on three structural components: pin-jointed rigid framing members, linear elastic sheathing panels, and nonlinear sheathing-to-framing connectors. The latter employed a hysteretic model which considered strength and stiffness degradation and pinching under cyclic loading. The model predicted accurately the force–displacement response and the energy dissipation of wood frame walls under general cyclic loads when compared to test results. The proposal was incorporated into a computer program called Cyclic Analysis of Shear Walls (CASHEW). A modified version of this model was later proposed by Pang and Hassanzadeh [18], who employed a corotational formulation and large-displacement theory to predict the collapse load and failure mechanism of both engineered and non-engineered wood frame shear walls. This new model was coded into a computer program called M − CASHEW. The model was verified by comparing its predictions with the data obtained for shear walls and diaphragms tested by previous researchers, showing good agreement even at large displacements. Casagrande et al. [19,20] developed an analytical tool to predict the elastic and elasto-plastic behavior of conventional wood frame walls under lateral and vertical load. Based on the results of a comprehensive parametric study, the authors proposed a rheological model as a function of the mechanical properties of the sheathing-to-framing connectors. Results showed good agreement between test data and model predictions for walls with different configurations. Seim et al. [4] developed a numerical model to study the nonlinear response of the strong walls tested in their experimental program (described in the previous section). The framing was represented by pin-jointed elastic beam-column elements, while the sheathing panels were modeled as an equivalent truss system with stiff boundary elements and elastic diagonals. For the sheathing-to-framing

Table 1
Mechanical properties for radiata pine framing and 11.1-mm-thick OSB panels obtained from testing.

Test	Framing members			OSB	
	Bending E (MPa)	Tensile σ_u (MPa)	Compression σ_u (MPa)	Along G_{LT} (MPa)	Across G_{LR} (MPa)
Number of tests	15	15	15	20	20
Mean	11399.73	26.54	34.78	1307.49	1255.66
SD	1811.08	13.30	8.23	88.31	187.22

connections, zero-length springs with the MSTEW model were employed. The walls were fully anchored to the ground by restraining the vertical and lateral displacements of the bottom rail. Results showed good agreement between the model predictions and the test measurements, highlighting that the wall response can be assessed with relatively large accuracy only on the basis of the calibrated data of sheathing-to-framing connections.

Despite the exhaustive efforts that have been devoted to the nonlinear model of conventional wood frame walls, investigations on modeling approaches for strong walls are limited. Even though the different configuration of the strong wood frame walls does not change the overall system behavior when compared to conventional walls, the force and displacement demands are distributed differently among elements that make them up. Whilst in conventional walls the top displacement is mainly due to the deformation in the sheathing-to-framing connectors, in strong walls the anchoring system has a significant contribution to the lateral top displacement. This is because the deformation mechanism in wood frame walls has three major components: (1) the sheathing-to-framing connectors, (2) the flexural flexibility of the studs, and (3) the anchoring devices [21]. These components can be represented by three elements connected in series. In strong walls, the shear stiffness associated to the sheathing-to-framing connectors is high enough to induce significant deformations in the anchorage system when the wall is subjected to lateral forces. The contribution of such deformations to the global lateral displacement depends on the wall aspect ratio. As will be discussed later in this paper, wood frame walls with four different aspect ratios were investigated in this research (3.43, 2.0, 1.0, and 0.67). It was found that the percentage of lateral deformation due to wall uplift was, on average, 50.7%, 50.3%, 25.0%, and 7.1% for each aspect ratio, respectively. Interestingly, it can be noted that for slender walls, about half of the lateral deformation is due to uplift. This is due to the small distance between the pivot points at the ends of the wall, which increases the lever arm from the top, and provokes small uplifts to induce large lateral displacements. Therefore, traditional modeling approaches that consider a fixed base and ignore the anchoring system deformation, as in the CASHEW model, may not be applicable to reproduce the lateral behavior of strong walls.

Since accurate numerical models are crucial to promote the development of mid-rise timber buildings, this paper proposes an efficient approach for modeling strong wood frame walls. The proposed model was developed based on the efforts of the previously discussed investigations [4,17–20,22], and aiming at developing a more comprehensive approach that embraces walls with different aspect ratios, takes into account the effects of sturdy end studs, and incorporates the deformation demands on the anchoring system. The model was validated by statistically comparing its predictions with twelve real scale tests of strong wood frame walls with different characteristics. Additionally, in-depth analyses were conducted to better understand the nonlinear behavior of wood frame walls and to gain knowledge about strategies to improve their response under earthquake cyclic loads. The model follows a simplified approach, which lies between mechanistic lumped models and complex FEM models. This reduces both the computational costs and the necessary input parameters, which can be obtained easily from previously published research or through simple standard tests.

2. Experimental program

An exhaustive experimental program was conducted to characterize the behavior of framing studs, structural OSB panels, sheathing-to-framing connections, and strong wood frame walls of different configurations and aspect ratios. A brief description of the tests is presented in this section.

Framing tests consisted of mechanically graded Chilean MGP10 (Australian structural grade) radiate pine. In total, forty five studs were mechanically tested under bending, tensile, and compression loads (15 specimens each) at the facilities of the INFOR Structural Wood Laboratory, Concepción, Chile, according to the Chilean standard NCh3028/1 [23]. Additionally, twenty OSB specimens (11.1 mm thick and made of radiate pine strands) were tested according to the ASTM D2719 standard [24] at the facilities of the Engineered American Wood Association (APA) in Tacoma, WA, USA, to determine their shear modulus in both the longitudinal and transverse directions. The mean results of framing and structural panels testing are listed in Table 1. The results are consistent with those reported in the literature [17,25,26]. Documentation of the testing program and further details of the experimental results can be found in [27].

The monotonic and cyclic behavior of the sheathing-to-framing connections was examined at the University of the Bío-Bío in Concepción, Chile. Double shear OSB-radiate pine framing joint specimens were pneumatically driven with 70-mm-long spiral nails with a shank diameter of 3.0 mm. Both directions (parallel and perpendicular to framing grain) were analyzed in each monotonic test, whilst all cyclic ones were conducted parallel to fiber direction. The yielding displacement obtained in the monotonic tests was used to compute the CUREE-Caltech cyclic testing protocol [28]. Fig. 2 shows an illustration of the testing set up and the monotonic and cyclic results for one specimen. Results are consistent with those reported in previous investigations [4,17,29,30], mainly in terms of capacity, stiffness, ductility, and energy dissipation, exhibiting a pinched response under reversed load for large displacements. Typical failure mechanisms were observed in the tests, such as yielding and fatigue failure of nails, nails being pulled out, or crushing of the OSB panel. A detailed report of the results can be found in [31].

To evaluate the overall behavior of strong wood frame walls, nineteen real scale specimens were tested as part of this research under monotonic and cyclic in-plane shear load. The walls were 2470 mm

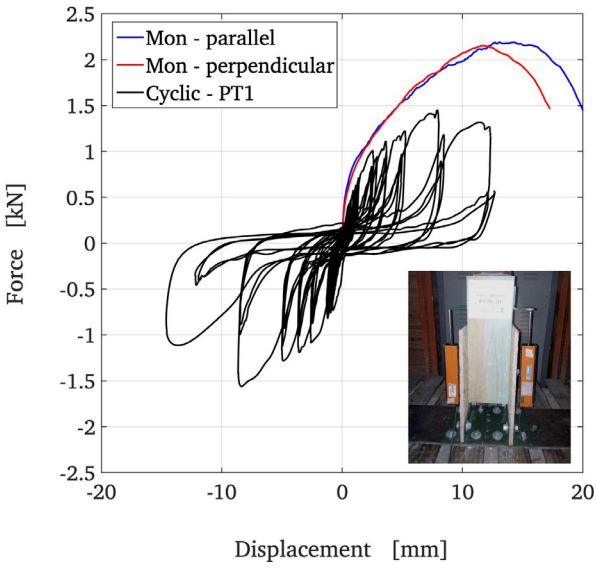

Fig. 2. Sheathing-to-framing connection test setup and results.

Fig. 3. Test setup (front and right view) for a 1200 mm long strong wall, labelled as C120-10-01 by Guiñez et al. [6].

high with four different lengths: 700, 1200, 2400, 3600 mm. All framing materials were 38 × 135 mm (2″ × 6″) dimensional lumber, and studs were spaced at 407 mm on center. The top and bottom plate consisted of double members, whereas the end studs had three members (for the 700 mm long walls) and five members (for the 1200, 2400 and 3600 mm long walls), respectively. 11.1 mm thick OSB panels were installed on both sides of the walls, employing 70 mm long spiral nails (3.0 mm shank diameter) spaced at 50 or 100 mm along all panel edges and at 200 mm for interior studs. SIMPSON Strong-Tie HD12 hold-down anchorages were bolted with four φ1 × 10″ horizontal bolts to the end studs and with one φ1-1/8 × 10″ bolt to the foundation. Additionally, φ1 × 10″ shear bolts were installed to prevent sliding of the wall. Four 1200 mm and three 2400 mm long walls were tested monotonically, and two 700 mm, four 1200 mm, four 2400 mm and two 3600 mm long walls were tested cyclically. The results of the monotonic tests and the guidelines provided by the ASTM E2126 standard [32] were used to calibrate the CUREE-Caltech protocol [28] for the cyclic tests. The test setup is shown in Fig. 3. A detailed report of the experimental program can be found in Guíñez et al. [6].

3. Nonlinear modeling approach

To better understand the nonlinear behavior of walls under large displacements, a new nonlinear model which takes into account the different deformation mechanisms in a wood frame wall was developed. Similar to Pang and Hassanzadeh [18], three types of elements were used to represent the wall assemblies: (1) 6-DOF planar-frame (beam) elements for the framing members, (2) 5-DOF shear-panel elements for the sheathing panels, and (3) 3-DOF link elements for sheathing-to-framing connections and hold-down devices. Since the nonlinear behavior of wood frame walls is dominated by the force-deformation characteristics of the sheathing-to-framing connections, the nails were modeled using nonlinear hysteretic springs, whereas the framing, sheathing members, and hold-down devices were assumed to be linear and elastic. The model was developed in the MATLAB M−CASHEW [18] environment.

3.1. Model description

Wood frame shear walls generally consist of six basic structural components: (1) framing members (i.e., interior studs, end studs, and top and bottom plates), (2) framing-to-framing connectors, which join studs with top and bottom plates, (3) sheathing-to-framing connectors, (4) sheathing OSB panels, (5) hold-down anchorage devices, and (6) shear bolts. Frame members were modeled using two-node Euler-Bernoulli frame elements with corotational formulation and 3 DOFs per node: two translational and one rotational. In the experiments, the framing elements for the end studs and top and bottom plates were bonded using high-quality structural glue, so that they behaved as a single member under large deformations. Hence, in the nonlinear model, these elements were represented by a single frame element considering the total width of all the studs, as shown in Fig. 4. Based on the results from the previous bending tests, a mean value of $E = 11.4$ GPa was considered for the studs.

Following the general practice in wood frame construction, only nominal nailing to hold the frame together was used in the tested walls, i.e., three 3 × 100 mm nails per joint. As the contribution of this connection type to the overall stiffness of the wall is small, its effect can be neglected [4,17]. Therefore, framing-to-framing connections (framing nails) were modeled as pin-ended connections using two-node 3-DOF link elements with two infinitely rigid springs for translation and one with zero stiffness for rotation. Sheathing-to-framing connectors (edge and field nails) were also modeled using two-node 3-DOF link elements, as discussed in detail in the following section. Sheathing OSB panels were modeled using rectangular shear-panel elements with 5 DOFs; one rigid-body rotation, two rigid-body translations, and two in-plane shear angles. Shear panels and frame elements were fastened together by the sheathing-to-framing connectors. From the OSB shear tests, an average value of $G = 1.3$ GPa was selected as the input shear modulus for the model.

The response of the hold-down system is the result of a complex combination of the behavior of the wooden members, the steel bolts, and the anchorage bar. Therefore, it is a common practice that the load-deformation response of hold-downs is represented by a nonlinear hysteretic model which captures its overall behavior [18,33]. However, if high capacity hold-down models are used (e.g., SIMPSON Strong-Tie HBD models with low-deflection performance), it is reasonable to assume that their response falls into the linear range. As it will be shown later in this paper, the demands on the hold-downs remain well under their maximum tensile capacity. Therefore, a linear 3-DOF link element that fixes the bottom plate to the base was used to represent the hold-down response. The vertical translational spring had a tensile stiffness of $k_t = 11.85$ kN/mm, which was determined based on the allowable tensile and deflection data provided by the design catalog [34], and a high compression stiffness to simulate the contact between the bottom plate and the foundation. The horizontal translational spring was also infinitely rigid to prevent sliding of the wall, whilst the rotational spring had zero stiffness. Finally, additional 3-DOF link elements were included to simulate the action of the shear bolts, preventing the sliding of the wall by assigning them an infinity horizontal stiffness. A detailed

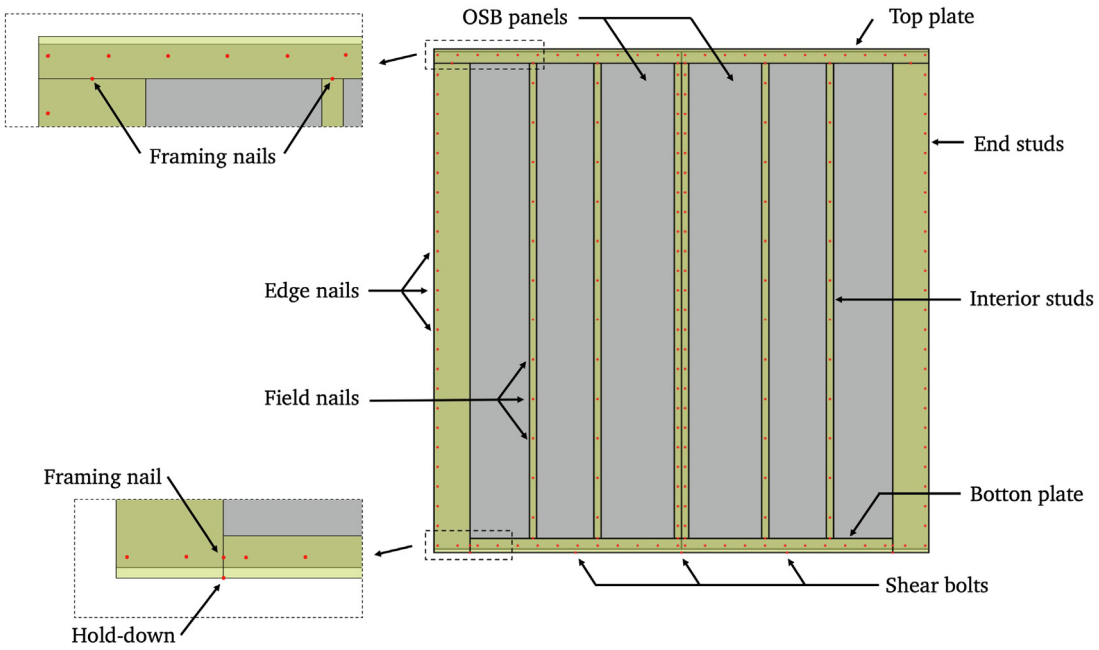

Fig. 4. Nonlinear model of a 2400 mm long wall.

description of the model formulation, connectivity, deformed geometry, and equilibrium equations of the elements can be found in Pang and Hassanzadeh [18].

3.2. Model calibration for sheathing-to-framing connections

The force–deformation behavior of nail connections is highly nonlinear under monotonic loading and exhibits a pinched hysteretic behavior with strength and stiffness degradation under cyclic loading [35]. Despite the existence of fairly sophisticated finite-element models which represent individual connectors as an elastoplastic pile embedded in a layered nonlinear foundation [33,36,37], each connection was modeled with three orthogonal uncoupled springs to achieve reasonable computational overheads in this research. Hence, the load-deformation response of each connection was represented by a hysteretic model based on a minimum number of path-following rules. The modified Stewart hysteretic model (MSTEW) proposed by Folz and Filiatrault [17] was adopted in this paper. Previous research has demonstrated the accuracy of the MSTEW model in representing the nonlinear response of sheathing-to-framing connections and wood frame walls [17,22,38,39].

The MSTEW model consists of 10 modeling parameters which phenomenologically capture the crushing of the wood (framing and sheathing) along with yielding of the nails. As depicted in Fig. 5(a), the nonlinear backbone envelope curve of the model is represented by the following set of equations:

$$F(\delta) = \mathrm{sgn}(\delta) \times (F_0 + r_1 K_0 |\delta|) \times [1 - \exp(-K_0 |\delta| / F_0)] \; |\delta| \leqslant |\delta_u|$$
$$F(\delta) = \mathrm{sgn}(\delta) \times F_u + r_2 K_0 [\delta - \mathrm{sgn}(\delta) \times \delta_u] \; |\delta_u| \leqslant |\delta| \leqslant |\delta_F|$$
$$F(\delta) = 0 \; |\delta| > |\delta_F|$$

Under cyclic loading, unloading off the envelope curve follows a path with a stiffness $r_3 K_0$. At this point, both the connector and wood are assumed to unload elastically. Under continued unloading, the response adopts a reduced stiffness $r_4 K_0$. Detailed information on the MSTEW model can be found in Folz and Filiatrault [17].

Through nonlinear functional minimization procedures and based on the average data from the sheathing-to-framing connection tests published by Jara and Benedetti [31], the 10 modeling parameters of the MSTEW model were identified for this research, and the results of the adjusted SDOF model are shown in Fig. 5(b). The values of the 10 parameters are shown in Table 2. Results from Folz and Filiatrault [17] for the connection tests carried out by Durham et al. [40] are also listed in Table 2 for comparison.

Good agreement is observed between the test and the MSTEW model, with an error in the cumulative energy dissipation (calculated as the area enclosed by the hysteresis cycles) of 4.2%. In the wood frame walls models, 3-DOF link elements were used to model sheathing-to-framing connections by employing three uncoupled springs: two translational and one rotational, as shown in Fig. 5(b). Each translational spring was assigned the MSTEW hysteretic model previously described. Since the rotational stiffness has a negligible effect on the response and behavior of the connection, the rotational spring was assigned a linear model with zero stiffness. On the other hand, previous research has shown that employing a pair of non-oriented springs (which keep a constant orientation) to represent sheathing connections overestimates the initial stiffness and the ultimate capacity of the shear walls [17,22]. To avoid this issue, the true oriented (corotation) connection model proposed by Pang and Hassanzadeh [18] was employed in this work.

3.3. Model validation

This section validates the accuracy of the proposed model when predicting the overall force-displacement response of strong wood frame walls with varying aspect ratios under different loading scenarios. Out of the total nineteen walls tested in the experimental program [6], twelve walls with four different aspect ratios and distinct responses were selected to explore the validity of the model. Four monotonic and eight cyclic tests were selected to demonstrate the accuracy of the model under different conditions for walls ranging from 700 mm to 3600 mm in length. For clarity purposes, the same specimen labeling of Guiñez et al. [6] has been adopted in this paper. For instance, the label M120-10–01 denotes the monotonic test of a 1200 mm long wall, with nail spacing of 100 mm, specimen number one. Monotonic results (test data and model predictions) for 1200 mm and 2400 mm walls are shown in Fig. 6. Monotonic analyses (pushover) were conducted by applying displacement in 0.5 mm increments. A norm displacement increment test [18] was used as the convergence criteria, with a residual tolerance of 1e-6 kN and 20 maximum iterations per increment. Analyses were stopped when the maximum force

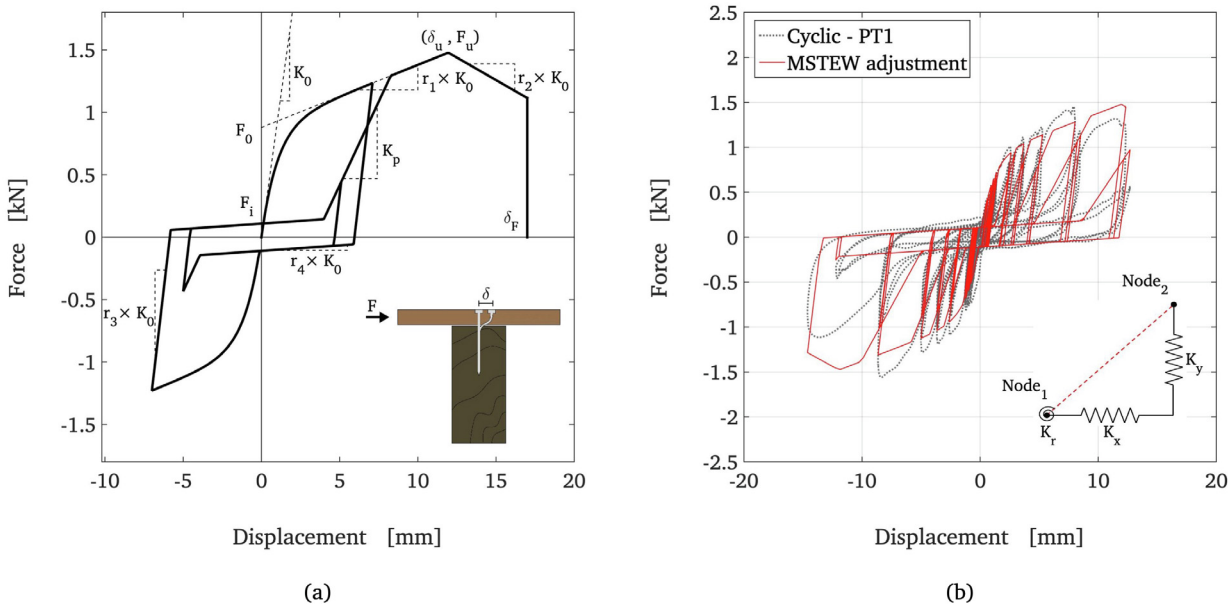

Fig. 5. MSTEW (a) model description and (b) prediction for sheathing-to-framing test PT1.

Table 2
MSTEW modeling parameters for sheathing-to-framing connections.

Case	MSTEW parameters									
	K_0 (kN/mm)	r_1	r_2	r_3	r_4	F_0 (kN)	F_I (kN)	δ_u (mm)	α	β
Current research	0.911	0.055	−0.079	1.177	0.010	0.879	0.109	11.951	0.569	1.165
Folz and Filiatrault [17]	0.561	0.061	−0.078	1.400	0.143	0.751	0.141	12.500	0.800	1.100

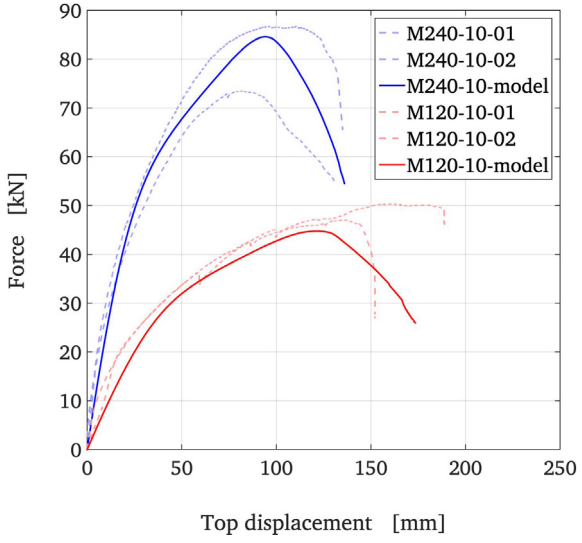

Fig. 6. Comparison between monotonic test results and model predictions for 1200 mm and 2400 mm long walls.

dropped by 40% or when the algorithm was no longer able to reach convergence.

Fig. 6 shows good agreement between the tests results and model predictions for 1200 mm and 2400 mm long walls. Monotonic tests were only conducted on these two walls. The M240-10–02 specimen showed a low maximum capacity, probably due to construction issues or poor nailing procedure. However, the model showed good accuracy when compared with the M240-10–01 test regarding wall capacity, stiffness, and ductility. The same was found for both 1200 mm walls.

In addition to four monotonic tests, eight cyclic analyses were conducted to prove the accuracy of the model under a reversed loading path. The top displacement data obtained from the test measurements were used as input in the control displacement analyses, and the results for four specimens are shown in Fig. 7. In general, good agreements between the test results and model predictions were observed for cyclic tests. The characteristic properties of nonlinear behavior, such as force and stiffness degradation and pinching, were fully captured by the model. It should be highlighted that the model is capable of estimating the wall response reasonably well for a wide range of aspect ratios (i.e. for 700 mm, 1200 mm, 2400 mm, and 3600 mm long walls), reaching good accuracy when predicting the reversed load-slip response.

For a detailed assessment of the proposed model, a quantitative comparison between test results and model predictions was also carried out for the selected twelve walls. Six engineering parameters were established as benchmarks for the evaluation: (1) maximum force F_{max}, (2) maximum displacement D_{max}, (3) initial stiffness K_0, (4) ultimate displacement D_u, (5) ductility μ, and (6) energy absorbed E_{abs}. The D_u value was estimated as the corresponding displacement to a force degradation of 20% (i.e., 0.8 F_{max}). When estimating the ductility, the yield force and displacement were calculated based on the equivalent energy elastic–plastic (EEEP) approach, according to the ASTM E2126 standard [32]. The EEEP approach is defined as an elastic–plastic plot with the same area enclosed by the force-displacement curve, with the elastic stiffness defined at 0.4 F_{max}. For the monotonic analyses, the benchmark parameters can be obtained directly from the test and model results. For the cyclic analyses, a positive and a negative envelope was calculated for each force-displacement relationship, and the mean envelope was obtained as the average of both, up to the D_u displacement. Then, the aforementioned parameters were obtained from

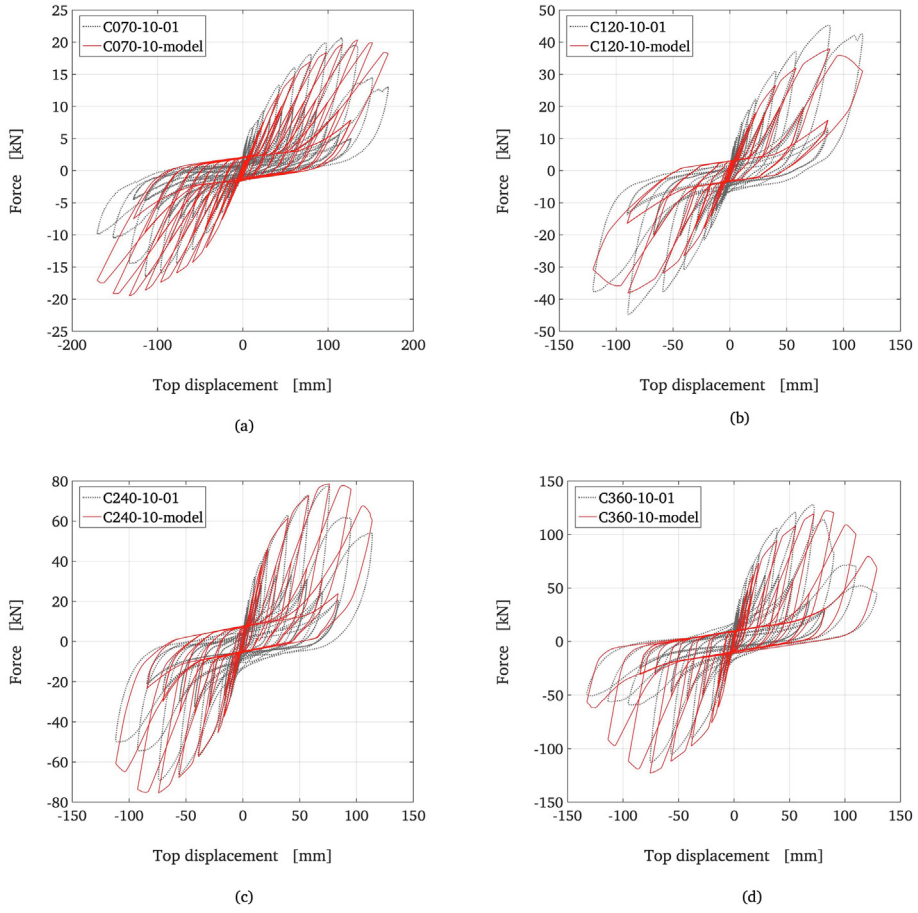

Fig. 7. Cyclic behavior of strong wood frame walls. Comparison between experiments and model predictions for the specimens: (a) C070-10-01, (b) C120-10-01, (c) C240-10-01 and (d) C360-10-01.

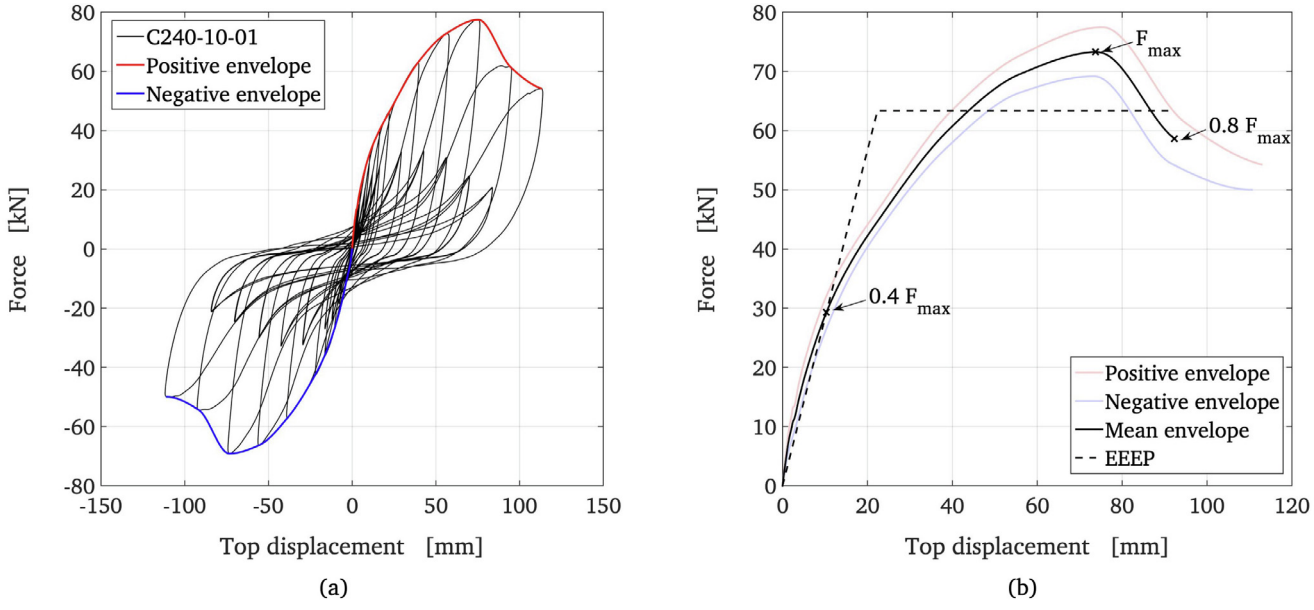

Fig. 8. Calculation of (a) cyclic envelopes and (b) EEEP curve for 2400 mm long wall results.

the mean envelope, and the absorbed energy was calculated as the area enclosed by the hysteretic cycles. This process is shown in Fig. 8 for the specimen C240-10–01.

The quantitative evaluation of the proposed model was done by normalizing the parameters obtained from the numerical models to those from the experimental tests. Consequently, values greater than one indicate that the model overestimates the parameter, while values less than one show that the model underestimates it. In Fig. 9, the six normalized parameters for each wall specimen are summarized in boxplots. The top and bottom of each box are the 25th and 75th

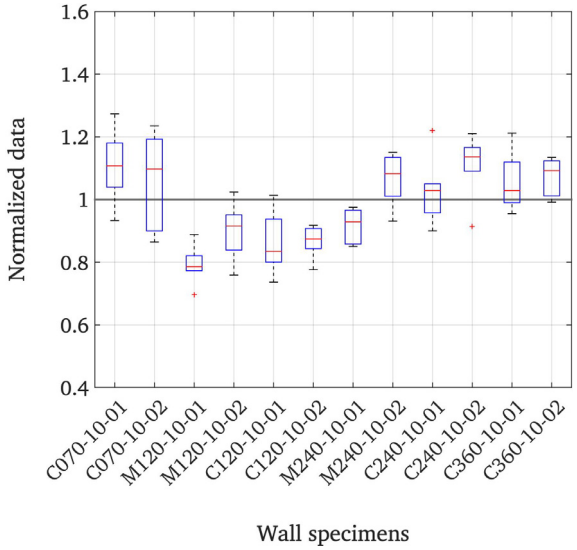

Fig. 9. Median values of the analyzed six parameters for each specimen.

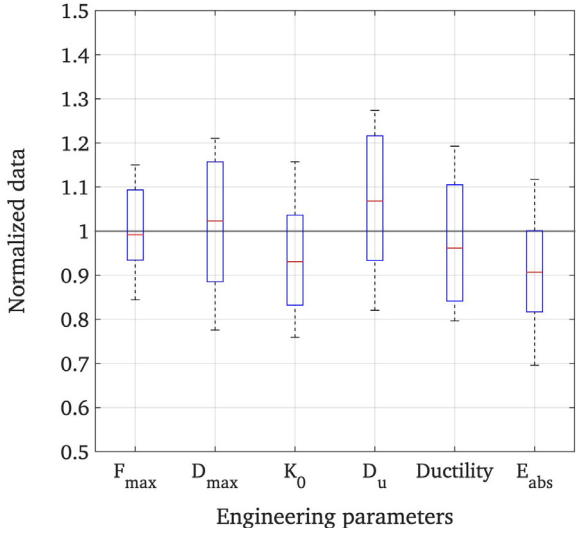

Fig. 10. Normalized data for each engineering parameter.

percentiles, respectively. The distances between the tops and bottoms are the interquartile ranges. The red line in the middle of each box is the median, and when it is not centered in the box, it shows data skewness. Whiskers are plotted from the ends of the interquartile ranges to the furthest values, and data beyond the whisker length are marked as outliers (red cross). A data point was identified as an outlier if it is more than 1.5 times the interquartile range away from the top or bottom of the box.

Fig. 9 shows reasonable agreements between tests results and model predictions, with errors within the allowable range considering the inherent wood material properties' variation, as listed in Table 1. The highest median value is 1.14 for the specimen C240-10-02 due to an overestimation of about 20% of D_{max} and D_u, while the lowest median value is 0.79 for the specimen M120-10-01. However, the mean value of the medians is 0.99 with a standard deviation of 0.12, which seems reasonable for nonlinear modeling under large displacements. The interquartile ranges (IQR) are useful when evaluating the data scattering. The largest IQR is 0.29 for the C070-10-02 wall, with 25th and 75th percentiles of 0.90 and 1.19, respectively. The lowest IQR value is 0.05 for the M120-10-01 wall, and the mean IQR for all specimens is 0.12.

For engineering purposes, it is interesting to analyze the capability of the proposed model when predicting the response of 1:1 walls (2400 mm long). This latter is relevant since it is a common practice to ignore walls with an aspect ratio greater than 2 (i.e., with length less than 1200 mm) in the lateral resistant system of wood frame buildings (interestingly, recent research has shown that high-aspect-ratio shear walls could have a positive influence on the building overstrength [41]). The medians for each 2400 mm long wall analyzed in this work are 0.93, 1.08, 1.03 and 1.14 respectively, with a mean of 1.04. The average IQR is 0.10. Despite these median values being close to 1 (i.e., a zero-error performance), results show some inaccuracy when predicting the D_u value for 1:1 walls. This is due to the complex phenomena that occur once the maximum capacity has been reached and the stiffness degradation begins; the crushing of the wood, failure of the OSB panels, nonlinear behavior of the anchorage system, tearing of sheathing-to-framing and framing-to-framing nails, could be associated with the discrepancy between the predictions and experimental data. Fig. 10 summarizes the accuracy of the model for each benchmark parameter analyzed, employing the data from all twelve specimens previously discussed and summarizing them in boxplots.

According to Fig. 10, the maximum force and displacement are well predicted by the model, with median values of 0.99 and 1.03. Furthermore, the remaining parameters also have close-to-one median values. The average of the medians is 0.98, and the average of the IQRs is 0.23. As a general trend, the energy absorbed tends to be underestimated by the model, with a median of 0.91 and 25th and 75th percentiles of 0.82 and 1.0, respectively.

Even though the modeling strategy proposed in this paper was developed to capture the intrinsic properties of strong wood frame walls, its generic approach allows it to be employed for predicting the lateral behavior of conventional walls as well. To prove the latter, one of the specimens tested by Durham et al. [40] at The University of British Columbia was modeled employing the methodology of this paper. The specimen corresponds to a shear wall commonly used in two-story wood frame houses. The test dimensions were 2400 × 2400 mm, i.e., a 1:1 wall. The framing material was 38 × 89 mm lumber, with studs spaced at 400 mm on center. The top plate and end studs were double members, whereas the bottom plate and the interior studs consisted of single members. To prevent overturning of the wall, conventional two-bolt corner hold-downs were installed, which also ensured a racking mode of deformation. The OSB sheathing panels were 9.5-mm-thick with an elastic shear modulus of 1.5 GPa and sheathed just one side of the wall. Three panels were used: a 1200 × 2400 mm panel for the bottom half of the wall and two 1200 × 1200 mm panels covered the top half of the wall. The sheathing-to-framing connections were pneumatically driven 50 mm long nails with a shank diameter of 2.67 mm. Nails spacing was 150 mm on center along all panel edges and 300 mm for all interior studs.

Fig. 11(a) shows the schematic of the nonlinear model developed for the test of Durham et al. [40], where the MSTEW modeling parameters originally proposed by Folz and Filiatrault [17] for sheathing-to-framing connections were employed (see Table 2). Fig. 11(b) depicts a comparison between the test result and model prediction under a cyclic loading path. As shown, the model predicts accurately the lateral force-displacement response of the wall for both small and large amplitude cycles in terms of stiffness and force, with an average error of 4.41% and 5.56%, respectively. It should be noted that the model does not capture properly the unloading stiffness. This results in an underestimation of the energy dissipated by the wall (16.05% error). This issue can be addressed by a better calibration of the r_3 parameter in the MSTEW model for the sheathing-to-framing connections. For instance, if $r_3 = 1.65$, the error reduces to 8.66% when predicting the dissipated energy.

It should be highlighted that the shear stiffness of conventional wood frame walls is lower compared to that of strong walls ($k_{strong}/k_{conventional} = 3.24$, calculated for $0.1F_{max}$) since they are built up with less OSB panels and sheathing-to-framing nails. Therefore, the

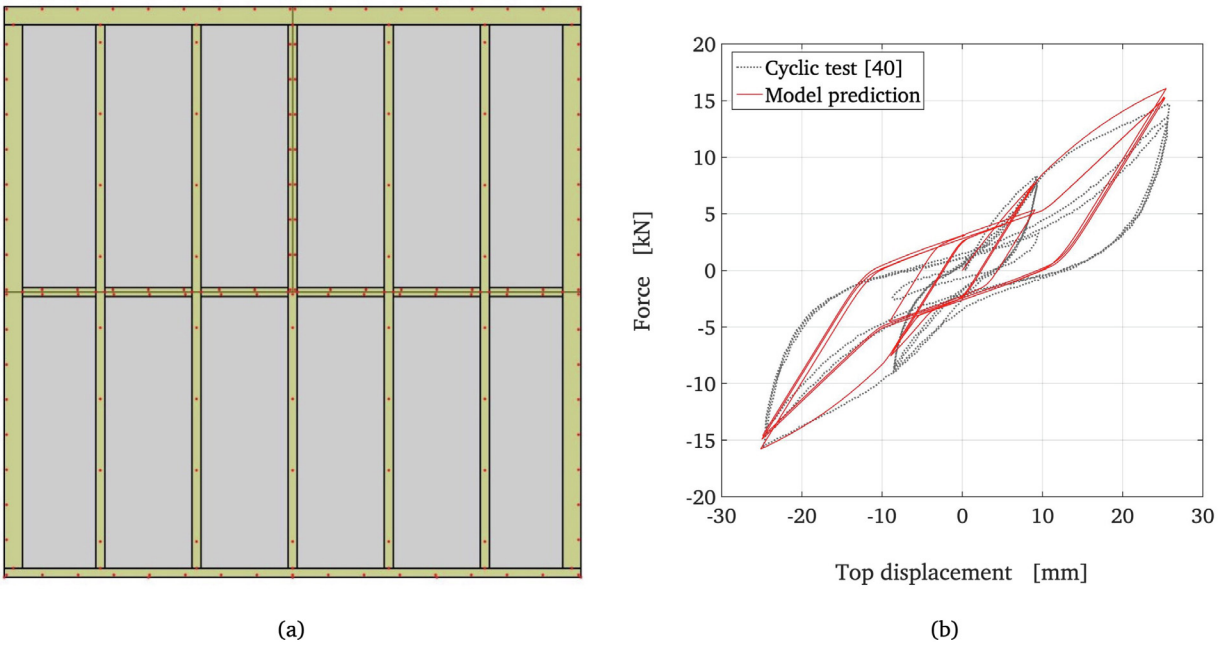

Fig. 11. Schematic of the wood frame wall tested by Durham et al. [40]: (a) modeling approach, (b) comparison between test results and model prediction.

deformation of the anchoring system is expected to reduce. This is due to the fact that the shear stiffness is not high enough to induce important demands in the hold-downs when the wall is subjected to lateral forces. Employing the model developed for the work of Durham et al. [40], the percentage of top lateral deformation due to wall uplift was estimated to be 10.02% for 1:1 conventional walls. This value is lower than the one for 1:1 strong walls (25.0%). Previous research has shown that for the vertical loads expected in the first floor of a typical two to four-story wood frame house (~25 kN/m), such small uplifts can be neglected, and that hold-down devices have minimal effect on the lateral behavior of walls [42,43].

4. Local response assessment

The proposed model was employed to conduct in-depth analyses of the nonlinear behavior of wood frame shear walls, and the results are discussed in this section. Even though FEM models (such as the one presented here) have computational overheads higher than simplified-mechanistic models, a relevant advantage is that they explicitly provide information about the response of each structural element (i.e., studs, nails, hold-downs, and panels). Such information is quite valuable for performance-based seismic design procedures, where nonlinear models that explicitly evaluate the local damage at the component level are needed.

4.1. Anchoring system

When evaluating the performance of wood frame walls, it is widely acknowledged that the damage level is related to the lateral drift or interstory drift. For instance, the FEMA 356 guidelines [44] establish three performance levels: immediate occupancy (IO), life safety (LS), and collapse prevention (CP), which are related to drifts of 1%, 2%, and 3%, respectively. However, these performance levels assume that all the damage is due only to shear deformation and that the wall is fully anchored. If the anchorage system (hold-down devices) fails, the wall loses its load-carrying capacity. Hence, analyzing the anchorage behavior in addition to the overall response of the wall could be relevant for large displacement demands. Fig. 12(a) shows the vertical load-deformation plot of the hold-down device of a 2400 mm long wall, obtained from the proposed numerical model. The tensile force was normalized by the allowable tensile capacity $T_{allowable}$ provided in the design catalog.

Fig. 12(a) shows the linear load-deformation response of the two-node link element employed to model the hold-down device in the lower-left corner of the wall. The maximum tensile force and displacement demand were 1.52 $T_{allowable}$ and 7.49 mm, respectively. In the design catalog, the allowable tension $T_{allowable}$ was determined as one-third of the maximum tension T_{ult}. Hence, the maximum tensile demand in the hold-down could be calculated as $1.52T_{allowable} = 0.51T_{ult}$. This means that the anchorage system remains below its failure capacity, and it justifies the assumption of assigning a linear elastic behavior to the hold-down. Furthermore, it is interesting to note that the load-slip relationship did not increase monotonically, but it unloaded after the wall reached its maximum capacity. This phenomenon can be observed in Fig. 12(b), where the wall top displacement was plotted versus force demand in the hold-down. The cross highlights the point where the wall reached its maximum capacity, which falls very close to maximum tensile force in the hold-down. At this point, the sheathing-to-framing connectors have reached their maximum capacities, and the stiffness degradation begins. Since the wall works as a series system, when there is a loss of stiffness in the sheathing-to-framing connectors, they experience greater deformations while the demand in the anchoring system reduces. This failure mechanism works as a safety switch that ensures a shear failure of the wall and prevents the hold-downs from pulling out. A similar phenomenon was found for walls with different aspect ratios, as depicted in Fig. 13. As noted by Schick and Seim [45], this highlights the importance of over-designing non-ductile elements (such as hold-downs) to ensure the ductile behavior of wood frame walls.

Interestingly, the tensile demands in the hold-downs remained low even for high aspect ratio walls. Therefore, the high contribution that the uplift has to the lateral top deformation in these walls is not due to higher tensile demands, but due to the slender geometry of the wall (i.e., small uplifts at the lower corners lead to large displacements at the top of the wall). On the other hand, the properties of the sheathing-to-framing connectors do have a considerable effect on the anchoring system demands. Fig. 14 shows the hold-down responses for a 2400 mm long wall which was modeled employing connections with different ductilities and maximum capacities.

For the results shown in Fig. 14(a), the hysteretic model of the

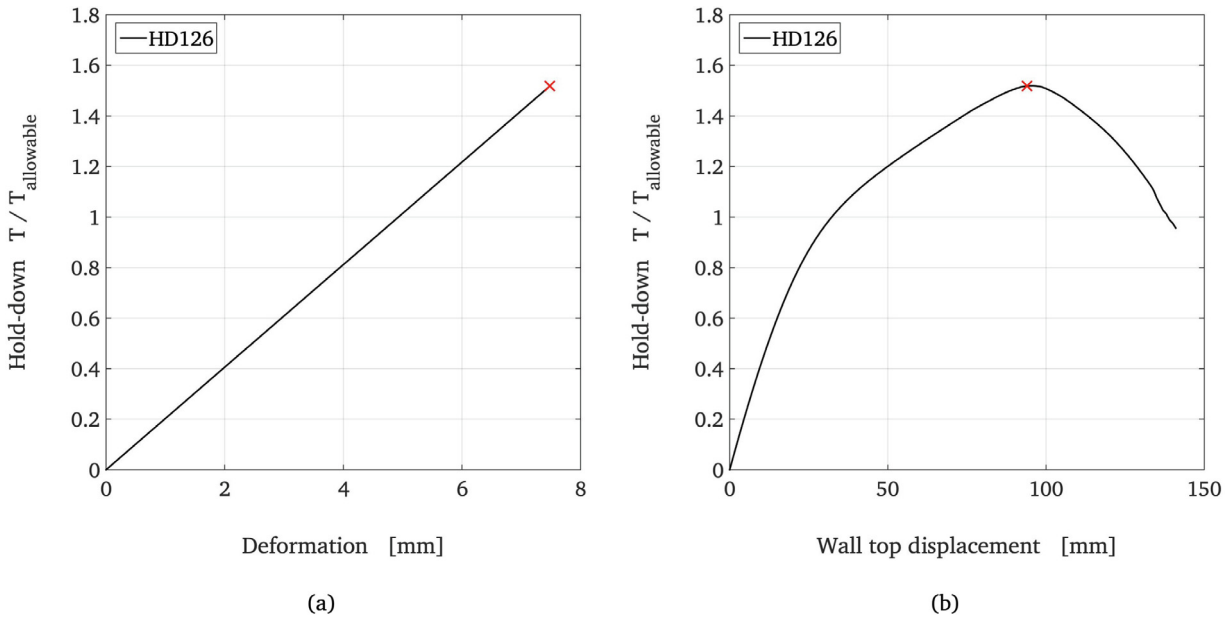

Fig. 12. Hold-down HD126 response in the strong shear walls system: (a) load versus hold-down deformation, and (b) load versus wall top displacement. The point where the wall reached its maximum capacity is highlighted with a red cross.

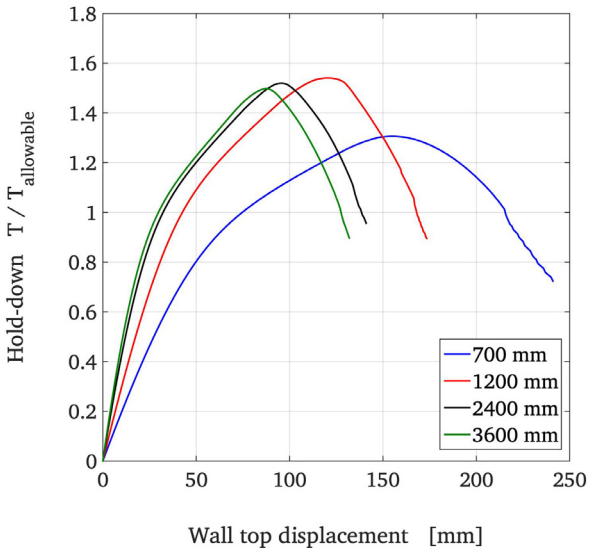

Fig. 13. Hold-down force demands for walls with different aspect ratios.

sheathing-to-framing connectors was modified so that it had the same maximum capacity but different values of ductility. For Fig. 14(b), the maximum capacity was modified, and the ductility was kept constant. As can be seen, an increment in ductility capacity did not increase the demand in the anchoring system, but only 'delayed' the point at which the maximum demand was reached. However, an increment in the maximum capacity of the sheathing-to-framing connectors raised the tensile force demands and may cause the failure of the hold-downs, as seen when F_{S2F} = 3.0 kN. Assuming that further failure mechanisms (such as shear buckling) do not take place, special care must be taken when designing the anchoring system if high-strength connectors, such as screws, are used in the wall design.

4.2. Sheathing-to-framing connectors

The deformation of sheathing-to-framing (S2F) connectors is due to the relative displacement between the OSB panels (sheathing) and the wood frame. Because of the rectangular geometry of the panels and the deformed configuration (racking mode) of the framing, the maximum deformation of a sheathing-to-framing connector depends on its position within the wall. Fig. 15(a) shows the maximum deformation field for a 2400 mm long wall calculated based on the results of a monotonic analysis. The data show that the S2F connectors located at the upper and lower corners and the central studs are prone to the greatest deformations. In other words, they contribute mostly to the resistance of the wall. Fig. 15(b) shows the percentage of energy absorbed by an S2F connector during a cyclic analysis as a function of its position within the wall. Similarly, the most demanded connectors are those at the upper and lower corners and the central studs. The S2F connectors placed at the interior studs have little contribution to the overall response of the wall, and their main function is to prevent the out-of-plane buckling of OSB panels. Based on the results described above, it is feasible to redesign the distribution of the S2F connectors within the wall, aiming at optimizing their location in the areas of greatest demand and increasing the capacity of the wall. An alternative design is proposed in Fig. 16(a) to demonstrate this.

For the optimization of the nailing pattern, the S2F connectors were concentrated at the upper and lower corners with a nail spacing of 50 mm, while at the intermediate zones the spacing was 150 mm. At the interior studs, a 300 mm spacing was selected. This meets the minimum requirement to the avoid out-of-plane buckling of OSB panels. In addition, the total number of connectors was kept constant before and after the optimization, i.e., 392. According to Fig. 16(b), the optimized wall had a 10% higher capacity than the original one, whilst the maximum displacement D_{max} remained almost the same (92.50 and 94.00 mm, respectively). However, a lower ductility was observed, due to a reduction in the ultimate displacement of the wall from 125.21 mm to 120.62 mm. When the S2F connectors are concentrated in the zones of greater demand, they reach the failure capacity simultaneously, reducing the post-peak residual capacity of the wall. It should be highlighted that although a non-uniform nailing pattern (such as the one presented above) may not be efficient for on-site constructions, it can be used in automated prefabrication processes to improve the cost-effectiveness of wood frame walls.

5. Simplified model for strong walls in multi-story buildings

Due to the structural complexity and large number of elements that

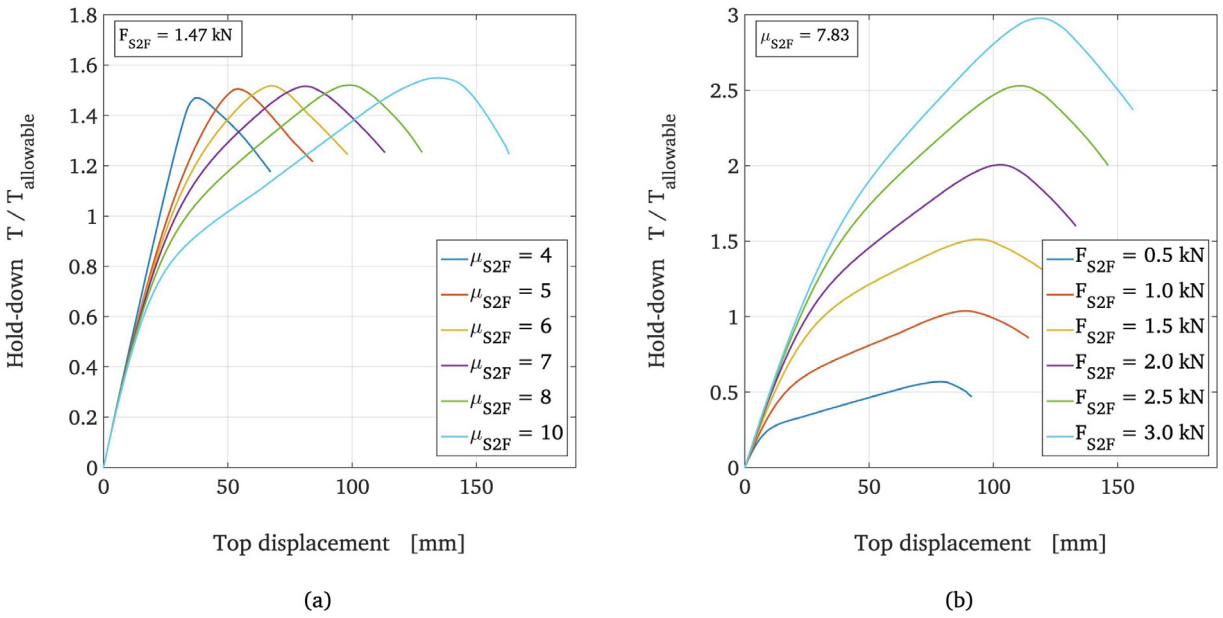

Fig. 14. Hold-down force demands for walls with different S2F (a) ductilities and (b) maximum capacities.

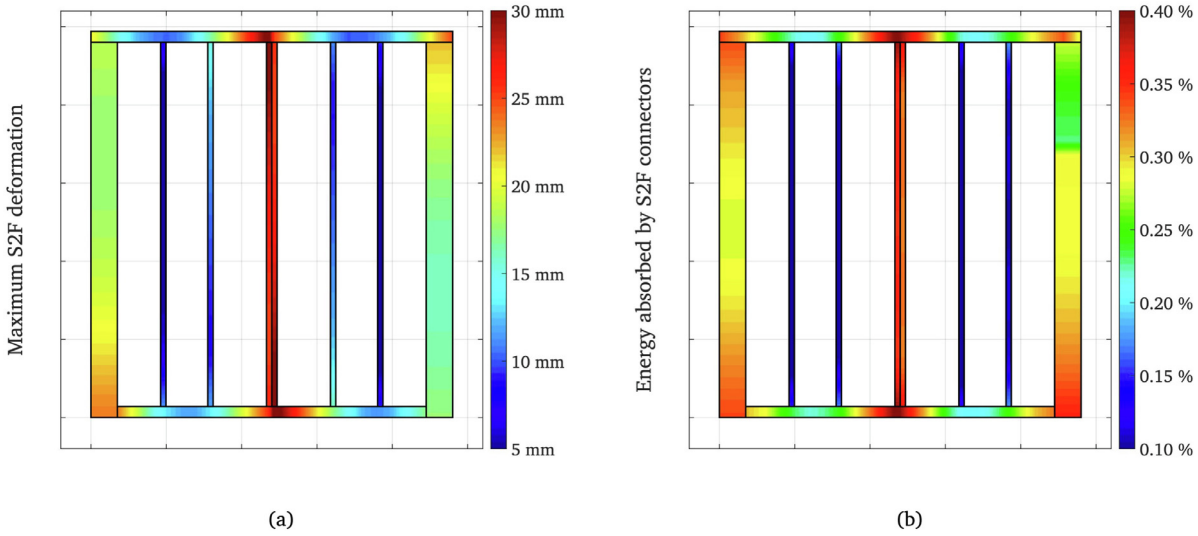

Fig. 15. Demands on sheathing-to-framing connectors: (a) deformation and (b) energy dissipation.

wood frame walls have, it is not feasible to develop detailed FEM models (as the one presented in this paper) for buildings with several stories. The computational and modeling effort involved in developing and analyzing such models would be quite intensive and thus limits their practical application. In contrast, simplified numerical models with reasonable accuracy levels are more attractive for practice engineers. Simplified lumped mass models which consider both the pure shear deformation [46] and the 'bending' deformation of the building [47] have been developed in the last few years, and they have been proven to work well when compared with test data [39,48]. In order to balance accuracy and computational overheads, these models represent the shear response of wood frame walls through nonlinear springs by employing hysteretic models that are capable of capturing the phenomena associated with the nonlinear behavior under large displacements, such as the MSTEW model [17] or the EPHM model [49]. Therefore, it is of relevant interest to determine the suitability of such models for strong wood frame walls as a necessary step towards studying the seismic behavior of mid-rise timber buildings using simplified approaches.

Employing the pure shear data from the diagonal measurements of a 2400 mm long wall (C240-10-01 specimen) during the test, a nonlinear spring was calibrated for the MSTEW model using a functional minimization procedure to estimate the model parameters, and the results are shown in Fig. 17. According to this figure, a single degree of freedom (SDOF) spring is able to reasonably capture the nonlinear behavior of the wall even for large displacements. As noted by Pei and van de Lindt [39], the model parameters K_0, F_0, and F_i that control force and stiffness can be scaled proportionally to the wall length. Consequently, the same set of MSTEW parameters can be used to predict the cyclic response of walls with the same nailing properties but of different lengths. Using the nonlinear model described in the previous section, the MSTEW parameters per unit length were calculated to predict the cyclic shear behavior of walls with different nailing patterns, and the results are listed in Table 3.

The data in Table 3 were calculated considering a field nail spacing of 200 mm, and assuming that the materials used for the walls have mechanical properties similar to those described in the experimental program of this project. Fig. 18 shows the accuracy of the MSTEW

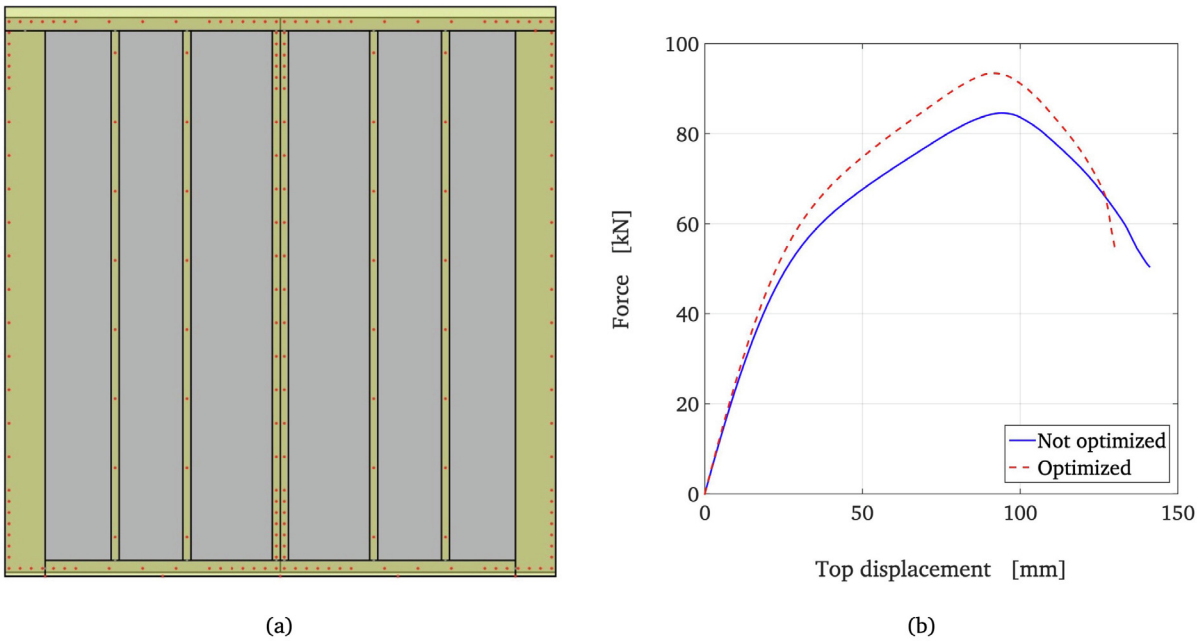

Fig. 16. Optimization of wood frame walls: (a) nailing pattern of the S2F connectors and (b) monotonic results before and after the optimization.

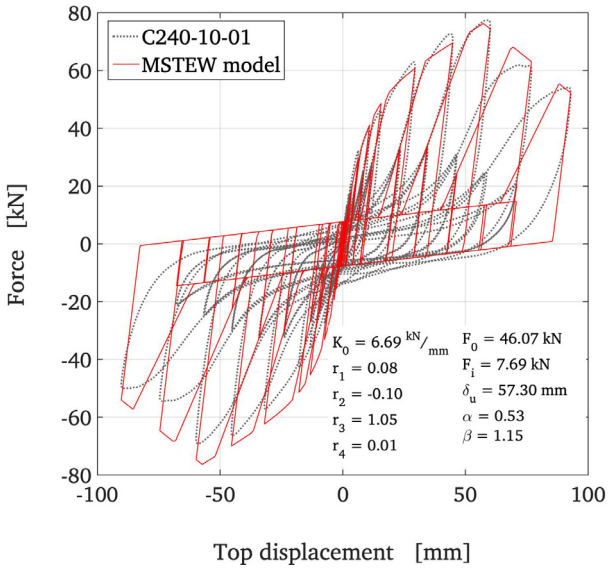

Fig. 17. Comparison between the test data and model predictions using the MSTEW model with adjusted parameters for the shear response of a 2400 mm long wall.

model to predict the shear response of walls with different lengths, using the data in Table 3 for double-OSB walls with an edge nail spacing of 100 mm. As can be seen, the MSTEW model works well when predicting the cyclic behavior of shear walls, achieving an acceptable degree of accuracy to be used in the nonlinear evaluation of wood frame buildings. In addition, considering that it is an SDOF model with a very low computational overhead, the cost-accuracy balance is adequate for the purpose pursued. It should be highlighted that, employing the data provided in Table 3, practicing engineers could also create simpler linear models for wood frame buildings in any commercial software (such as SAP2000, ETABS, RISA-3D, SAPWood, among others) and use them in force-based design methods, such as modal analysis or demand-capacity. Fig. 18 also shows a quantitative evaluation of the SDOF model using the previous six engineering parameters for each wall specimen. The normalized data are summarized in boxplots. The close-to-one results show a good performance of the model, with average values of the medians and IQRs of 0.97 and 0.15, respectively.

6. Conclusions

An efficient and accurate approach for monotonic and cyclic nonlinear modeling of strong wood frame shear walls is presented in this paper. Compared to models developed in previous investigations, this new approach aims at developing a more comprehensive approach that embraces walls with different aspect ratios, while taking into account the effects of sturdy end studs, and incorporating the deformation

Table 3
MSTEW parameters per unit length for modelling the shear response of strong wood frame walls.

Wall properties		MSTEW parameters									
OSB	Nail spacing [mm]	K_0 [kN/mm/m]	r_1	r_2	r_3	r_4	F_0 [kN/m]	F_i [kN/m]	δ_u [mm]	α	β
Single	50	2.374	0.072	−0.046	1.000	0.017	10.275	2.048	45.450	0.532	1.139
	100	1.393	0.079	−0.101	1.047	0.015	9.600	1.603	57.300	0.531	1.146
	150	1.080	0.079	−0.090	1.075	0.014	7.104	1.202	55.820	0.522	1.150
Double	50	2.487	0.097	−0.080	1.002	0.021	26.685	2.935	42.887	0.800	1.150
	100	2.786	0.079	−0.101	1.047	0.015	19.196	3.205	57.300	0.531	1.146
	150	2.159	0.079	−0.090	1.075	0.014	14.208	2.403	55.820	0.522	1.150

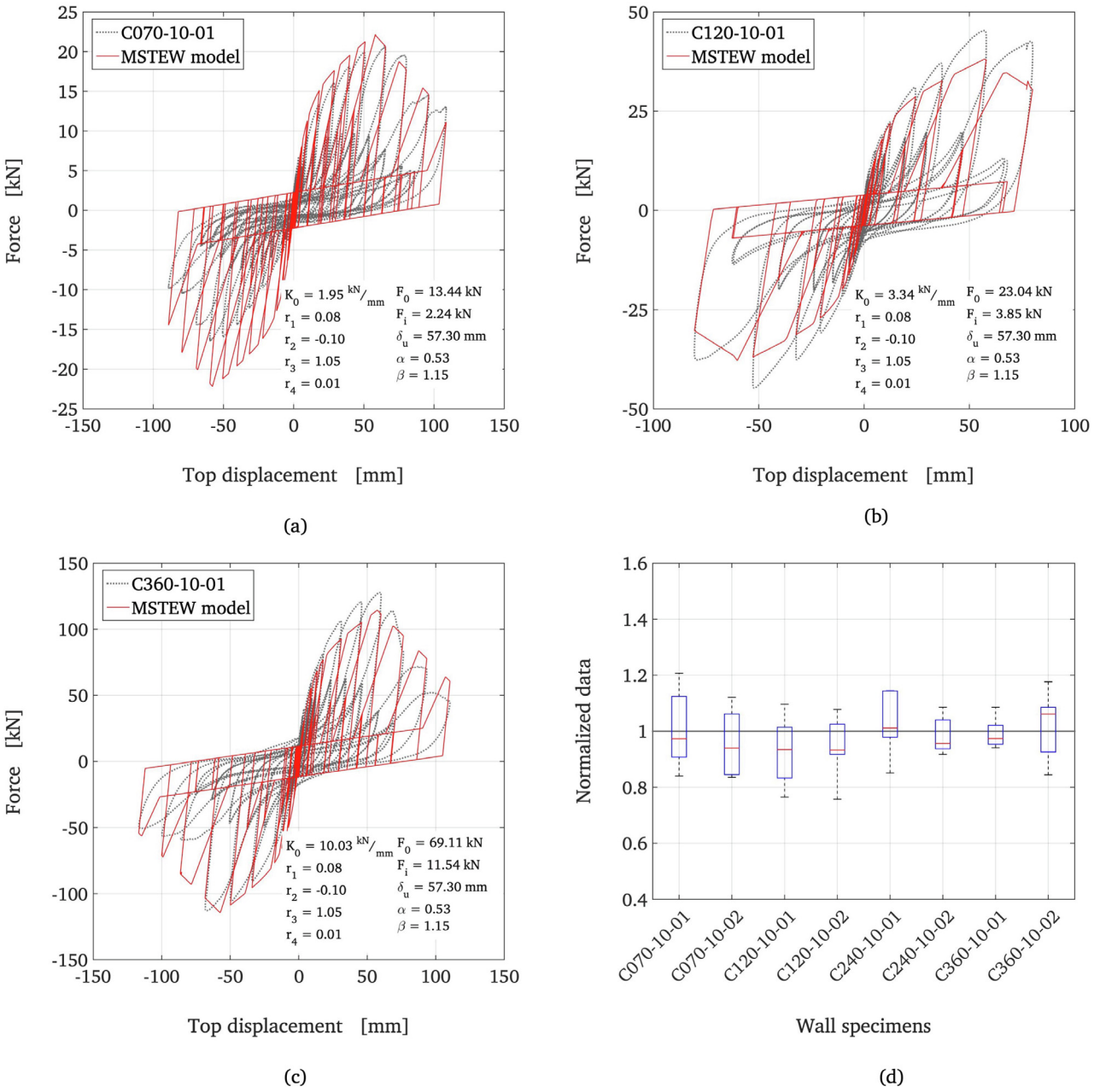

Fig. 18. MSTEW predictions for the shear response of (a) 700 mm, (b) 1200 mm, and (c) 3600 mm long walls, and (d) quantitative validation of the SDOF model.

demands in the anchoring system. The good agreements between the model predictions and the results from twelve real-scale experimental tests demonstrated that the proposed methodology is able to accurately reproduce the nonlinear response of a wide range of walls. Results also showed that complex phenomena such as force and stiffness degradation and pinching in strong walls could be captured reasonably well using the model. Furthermore, the model was used to conduct in-depth analyses of the nonlinear behavior of wood frame walls, which led to the following findings:

- The demands on the hold-downs in strong walls are relatively low (~0.51 T_{ult}). Hence, they are expected to behave in the linear range. Such demands do not increase monotonically, but they decrease after the wall reaches its maximum capacity. This phenomenon guarantees a shear failure and prevents the hold-downs from pulling out. Thus, the main failure mechanism of strong shear walls with code compliant aspect ratios is expected to be nail ductile shearing. Additionally, the design procedure of the hold-downs could be optimized to reduce the cost of the anchorage system.
- The mechanical properties of the sheathing-to-framing connectors have a significant effect on the anchoring system demands. Special care must be taken when designing wood frame walls if high-strength connectors (such as screws) are employed, since the load transfered to hold-downs could lead to their failure under large displacement demands.
- In strong wood frame walls with high aspect ratios, the percentage of global lateral deformation due to the uplift of the anchoring system is about 50%. This high contribution level is not due to great tensile demands, but to the slender geometry of the wall (i.e., small uplifts at the lower corners produce large displacements at the top of the wall). Based on such high rocking contributions to the wall deformation, yielding and ultimate drifts of strong shear walls may significantly increase.
- Due to the geometry of the OSB panels, the deformation demands

are concentrated at the upper and lower corners of the wall and the central studs. The contribution of the nails at the interior studs to the lateral capacity of the wall was found to be small.

- The nailing pattern can be optimized in wood frame walls to improve the performance of the wall without increasing the number of connections. It was shown that changing the nailing pattern can improve the maximum capacity of strong walls up to 10% at the price of slightly reducing ductility.
- The results of the presented numerical model can be used to calibrate a SDOF model. This simpler and easy-to-use model can then be employed to reproduce the nonlinear shear behavior of wood frame walls at a very low computational effort for further assessments. The SDOF model parameters can be normalized per unit length to predict the pure shear response of walls with similar nailing patterns but of different wall lengths. This simpler model is intended to make the nonlinear modeling of mid-rise timber structures efficient, guide earthquake engineers in practice, and provide valuable information for both force-based [50–52] and performance-based [53,54] seismic design procedures for multi-story wood frame buildings.

CRediT authorship contribution statement

Xavier Estrella: Conceptualization, Investigation, Methodology, Software, Validation, Writing - original draft, Writing - review & editing. **Pablo Guindos:** Conceptualization, Resources, Supervision, Writing - review & editing, Funding acquisition. **José Luis Almazán:** Conceptualization, Resources, Methodology, Supervision, Writing - review & editing. **Sardar Malek:** Conceptualization, Methodology, Formal analysis, Supervision, Writing - review & editing.

Declaration of Competing Interest

The authors declared that there is no conflict of interest.

Acknowledgments

The authors would like to recognize the financial support provided by CONICYT (Doctorado Nacional 2019 – 21191267), VRI-UC, and UTS Graduate Research School. The authors also thank Jairo Montaño and Professor Keith Crews for their valuable support and constructive comments during the course of this research.

References

[1] Follesa M, Fragiacomo M, Casagrande D, Tomasi R, Piazza M, Vassallo D, et al. The new provisions for the seismic design of timber buildings in Europe. Eng Struct 2018;168:736–47. https://doi.org/10.1016/j.engstruct.2018.04.090.
[2] Jayamon J, Line P, Charney F. State-of-the-art review on damping in wood-frame shear wall structures. J Struct Eng 2018;144:1–13. https://doi.org/10.1061/(ASCE)ST.1943-541X.0002212.
[3] van de Lindt J, Pei S, Pryor S, Shimizu H, Isoda H. Experimental seismic response of a full-scale six-story light-frame wood building. J Struct Eng 2010;136:1262–72. https://doi.org/10.1061/(asce)st.1943-541x.0000222.
[4] Seim W, Kramar M, Pazlar T, Vogt T. OSB and GFB as sheathing materials for timber-framed shear walls: comparative study of seismic resistance. J Struct Eng 2016;142:E4015004. https://doi.org/10.1061/(ASCE)ST.1943-541X.0001293.
[5] Sadeghi Marzaleh A, Nerbano S, Sebastiani Croce A, Steiger R. OSB sheathed light-frame timber shear walls with strong anchorage subjected to vertical load, bending moment, and monotonic lateral load. Eng Struct 2018;173:787–99. https://doi.org/10.1016/j.engstruct.2018.05.044.
[6] Guíñez F, Santa María H, Almazán JL. Monotonic and cyclic behaviour of wood frame shear walls for mid-height timber buildings. Eng Struct 2019;189:100–10. https://doi.org/10.1016/J.ENGSTRUCT.2019.03.043.
[7] Easley J, Foomani M, Dodds R. Formulas for wood shear walls. J Struct Div 1982;108:2460–78.
[8] Itani R, Cheung C. Nonlinear analysis of sheathed wood diaphragms. J Struct Eng 1984;110:2137–47.
[9] Gutkowski R, Castillo A. Single- and double-sheathed wood shear wall study. J Struct Eng 1988;113:241–59.
[10] Dolan J. The dynamic responses of timber shear walls. Ph.D. Dissertation, Faculty of Civil Engineering. Vancouver, Canada: University of British Columbia; 1989.
[11] Dolan J, Foschi R. Structural analysis model for static loads on timber shear walls. J Struct Eng 1991;117:851–61.
[12] White M, Dolan J. Nonlinear shear-wall analysis. J Struct Eng 1995;121:1629–35.
[13] Xu J, Dolan J. Development of a wood-frame shear wall model in ABAQUS. J Struct Eng 2009;135:977–84. https://doi.org/10.1061/(asce)st.1943-541x.0000031.
[14] Filiatrault A. Static and dynamic analysis of timber shear walls. Can J Civ Eng 1990;17:643–51.
[15] Gupta A, Kuo G. Wood-framed shear walls with uplifting. J Struct Eng 1987;113:241–59.
[16] Seible F, Filiatrault A, Uang C. Workshop on Seismic Testing, Analysis and Design of Woodframe Construction. Proc. Invit. Work. Seism. Testing, Anal. Des. Woodframe Constr., Richmond, CA: 1999.
[17] Folz B, Filiatrault A. Cyclic analysis of wood shear walls. J Struct Eng 2001;127:433–41.
[18] Pang W, Hassanzadeh S. Corotational model for cyclic analysis of light-frame wood shear walls and diaphragms. J Struct Eng 2012;139:1303–17. https://doi.org/10.1061/(asce)st.1943-541x.0000595.
[19] Casagrande D, Rossi S, Sartori T, Tomasi R. Proposal of an analytical procedure and a simplified numerical model for elastic response of single-storey timber shear-walls. Constr Build Mater 2016;102:1101–12. https://doi.org/10.1016/j.conbuildmat.2014.12.114.
[20] Casagrande D, Rossi S, Tomasi R, Mischi G. A predictive analytical model for the elasto-plastic behaviour of a light timber-frame shear-wall. Constr Build Mater 2016;102:1113–26. https://doi.org/10.1016/j.conbuildmat.2015.06.025.
[21] American Wood Council. Special design provisions for wind and seismic. ANSI/AWC SDPWS-2015, Leesburg, VA: 2015.
[22] Judd J, Fonseca F. Analytical model for sheathing-to-framing connections in wood shear walls and diaphragms. J Struct Eng 2005;131:345–52. https://doi.org/10.1061/(ASCE)0733-9445(2005)131:2(345).
[23] INN. Madera estructural. Determinación de propiedades físicas y mecánicas de la madera clasificada por su resistencia. Parte 1: Métodos de ensayo en tamaño estructural. NCh 3028/1-Of 2006. Instituto Nacional de Normalización, Santiago, Chile: 2006.
[24] ASTM. ASTM D2719-13: Standard test methods for structural panels in shear through-the-thickness. ASTM International, West Conshohocken, PA: 2013.
[25] Segura G. Determinación del módulo de corte de tableros de fibra orientada a través de ensayo de análisis modal. Bachelor's Dissertation, Department of Civil and Environmental Engineering, Universidad del BíoBío, Concepción, Chile, 2017.
[26] Cartes S, González M, Padilla J. Actualizar tensiones basicas admisibles de madera aserrada de pino radiata para uso de elementos laminados. Simp. Habilitación Prof., Concepción, Chile: 2017.
[27] INFOR. Ensayos de flexión, tracción y compresión a madera aserrada de Pino Radiata. Instituto Forestal, Concepción, Chile: 2017.
[28] Krawinkler H, Parisi F, Ibarra L, Ayoub A, Medina R. Development of a testing protocol for woodframe structures. CUREE Report W-02, Task 1.3.2, Consortium of Universities for Research in Earthquake Engineering, Richmond, CA: 2001.
[29] Sartori T, Tomasi R. Experimental investigation on sheathing-to-framing connections in wood shear walls. Eng Struct 2013;56:2197–205. https://doi.org/10.1016/j.engstruct.2013.08.039.
[30] Casagrande D, Bezzi S, D'Arenzo G, Schwendner S, Polastri A, Seim W, et al. A methodology to determine the seismic low-cycle fatigue strength of timber connections. Constr Build Mater 2020;231:117026https://doi.org/10.1016/j.conbuildmat.2019.117026.
[31] Jara A, Benedetti F. Informe No. 14 – Registro de estudio de ensayos de conectores. University of the Bío Bío, Concepción, Chile: 2017.
[32] ASTM. ASTM E2126-11: Standard test methods for cyclic (reversed) load test for shear resistance of vertical elements of the lateral force resisting systems for buildings. ASTM International, West Conshohocken, PA: 2018.
[33] Li M, Lam F, Yeh B, Skaggs T, Rammer D, Wacker J. Modeling force transfer around openings in wood-frame shear walls. J Struct Eng 2012;138:1419–26. https://doi.org/10.1061/(asce)st.1943-541x.0000592.
[34] Simpson Strong-Tie. Wood construction connectors. Simpson Strong-Tie Company Inc, Pleasanton, CA: 2015.
[35] Dolan J, Madsen B. Monotonic and cyclic nail connection tests. Can J Civ Eng 1992;19:97–104.
[36] Chui Y, Ni C, Jaing L. Finite-element model for nailed wood joints under reversed cyclic load. J Struct Eng 1998;124:96–103.
[37] Foschi R. Modeling the hysteretic response of mechanical connections for wood structures. Proc. 6th World Conf. Timber Eng., Whistler, Canada: 2000.
[38] Pang W, Rosowsky D, Pei S, van de Lindt J. Simplified direct displacement design of a six-story woodframe building and pretest seismic performance assessment. J Struct Eng 2010;136:813–25. https://doi.org/10.1061/(ASCE)ST.1943-541X.0000181.
[39] Pei S, van de Lindt J. Seismic numerical modeling of a six-story light-frame wood building: comparison with experiments. J Earthq Eng 2011;15:924–41. https://doi.org/10.1080/13632469.2010.544840.
[40] Durham J, Lam F, Prion G. Seismic resistance of wood shear walls with large OSB panels. J Struct Eng 2001;127:1460–6.
[41] Jayamon J, Line P, Charney F. Sensitivity of wood-frame shear wall collapse performance to variations in hysteretic model parameters. J Struct Eng 2019;145:1–12. https://doi.org/10.1061/(ASCE)ST.1943-541X.0002210.
[42] Dean P, Shenton H. Experimental investigation of the effect of vertical load on the capacity of wood shear walls. J Struct Eng 2005;131:1104–13. https://doi.org/10.1061/(asce)0733-9445(2005)131:7(1104).
[43] Johnston A, Dean P, Shenton H. Effects of vertical load and hold-down anchors on the cyclic response of wood framed shear walls. J Struct Eng 2006;132:1426–34. https://doi.org/10.1061/(asce)0733-9445(2006)132:9(1426).

[44] FEMA. FEMA 356: Prestandard and commentary for the seismic rehabilitation of buildings. Federal Emergency Management Agency, Washington, D.C.: 2000.
[45] Schick M, Seim W. Overstrength values for light frame timber wall elements based on reliability methods. Eng Struct 2019;185:230–42. https://doi.org/10.1016/j.engstruct.2019.01.034.
[46] Folz B, Filiatrault A. Seismic analysis of woodframe structures. I: model formulation. J Struct Eng 2004;130:1353–60. https://doi.org/10.1061/(asce)0733-9445(2004)130: 9(1361).
[47] Pei S, van de Lindt J. Coupled shear-bending formulation for seismic analysis of stacked wood shear wall systems. Earthq Eng Struct Dyn 2009;38:1631–47.
[48] Folz B, Filiatrault A. Seismic analysis of woodframe structures. II: model implementation and verification. J Struct Eng 2004;130:1361–70.
[49] Pang W, Rosowsky D, Pei S, van de Lindt J. Evolutionary parameter hysteretic model for wood shear walls. J Struct Eng 2007;133:1118–29. https://doi.org/10.1061/(asce)0733-9445(2007)133:8(1118).
[50] Rossi S, Casagrande D, Tomasi R, Piazza M. Seismic elastic analysis of light timber-frame multi-storey buildings: proposal of an iterative approach. Constr Build Mater 2016;102:1154–67. https://doi.org/10.1016/j.conbuildmat.2015.09.037.
[51] Seim W, Hummel J, Vogt T. Earthquake design of timber structures - Remarks on force-based design procedures for different wall systems. Eng Struct 2014;76:124–37. https://doi.org/10.1016/j.engstruct.2014.06.037.
[52] Hummel J, Seim W, Otto S. Steifigkeit und eigenfrequenzen im mehrgeschossigen holzbau. Bautechnik 2016;93:781–94. https://doi.org/10.1002/bate.201500105.
[53] van de Lindt J, Rosowsky D, Pang W, Pei S. Performance-based seismic design of midrise woodframe buildings. J Struct Eng 2013;139:1294–302. https://doi.org/10.1061/(ASCE)ST.1943-541X.0000653.
[54] Mergos P, Beyer K. Displacement-based seismic design of symmetric single-storey wood-frame buildings with the aid of N2 method. Front Built Environ 2015;1:1–11. https://doi.org/10.3389/fbuil.2015.00010.